Bioelectronic Noses

Polypyrrole Nanotubes Conjugated with Human Olfactory Receptors: High-Performance Transducers for FET-Type Bioelectronic Noses**

Hyeonseok Yoon, Sang Hun Lee, Oh Seok Kwon, Hyun Seok Song, Eun Hae Oh, Tai Hyun Park,* and Jyongsik Jang*

Significant advance in conducting polymers (CPs) has prompted the development of devices such as organic light-emitting diodes, solar cells, memories, and field-effect transistors (FETs). As alternatives to inorganic semiconductors or metals, CPs provide great potential to produce low-cost, large-area, lightweight, and flexible devices. Recently, CP nanomaterials have received considerable attention because of remarkable physical and chemical characteristics originating from their small dimensions and high surface area.[1] CP nanomaterials also inherit advantages such as facile functionalization and biocompatibility from their bulk counterparts.[2] Importantly, these features make CP nanomaterials highly attractive for various future applications. Typically, there is an increasing interest in the use of CP nanomaterials in analytical sciences.[3, 4]

Odor discrimination is a challenging research subject for key applications in the fields of foods and beverages, environmental monitoring, and disease diagnosis.[5] The challenges arise from the fact that only subtle differences in the molecular structure of an odorant can lead to pronounced modifications in odor quality. Human and animal noses can perceive more than hundreds of thousands of odor molecules.[6] Accordingly, particular attention has been paid to the development of sensors that mimic the mammalian olfactory system. A few significant studies regarding biotechnology-based olfactory sensors, which are called bioelectronic noses, have been reported, mainly based on quartz crystal microbalances.[7,8] However, their sensitivity and selectivity leave room for improvement.

Although CPs have been extensively implemented in different types of sensors,[9] the use of CP nanomaterials as

both transistor channel and sensitive element has been limited, owing to difficulties in their synthesis and manipulation. Herein, we describe the integration of human olfactory receptors (hORs) and CP nanotubes into a FET platform suitable for electronic control. Field-induced sensitivity was observed, eventually leading to the recognition of a target odorant at an unprecedentedly low concentration. To our knowledge, this is the first example of FET-type bioelectronic noses based on hOR-conjugated CP nanotubes.[10]

First of all, hOR 2AG1 (hOR2AG1) was expressed in *Escherichia coli* (*E. coli*) as a fusion protein with a glutathione-*S*-transferase (GST) tag at its N terminus.[8] The GST tag was used as a fusion partner for efficient expression and also for the Western blot analysis to confirm the expression of olfactory receptor protein. The *E. coli* cells were sonicated to obtain a membrane fraction. The hOR2AG1 was difficult to solubilize with detergents. In contrast, most of the impurity proteins were solubilized with Triton X-100 from the insoluble fraction. To remove membrane-integrated proteins other than hOR2AG1, the membrane fraction was treated with 5% triton X-100 and then retrieved by centrifugation. CP nanotubes were synthesized with the aid of cylindrical micelle templates in an apolar solvent.[11] Chemical copolymerization of pyrrole with pyrrole-3-carboxylic acid (P3CA) on the cylindrical micelle surface yielded intrinsically functionalized CP nanotubes (four-probe conductivity: 10^{-1}–$10^{0}\,\mathrm{S\,cm^{-1}}$), namely carboxylated polypyrrole nanotubes (CPNTs).

Figure 1a schematically shows the FET sensor platform based on hOR-conjugated CP nanotubes.[12] An interdigitated microelectrode array (IDA) was patterned on a glass substrate through a lithographic process. The IDA consisted of a pair of gold electrode bands with 25 fingers each, in which the bands served as source (S) and drain (D) electrodes, respectively. The IDA was 2 μm wide, 1 mm long, and had 2 μm interfinger gaps. CPNTs were immobilized on the electrode substrate through covalent linkages to maintain stable electrical contact between the nanotubes and the electrodes. The IDA substrate was treated with an aminosilane (3-aminopropyltrimethoxysilane, APS), and the carboxy functional groups of the CPNTs were then coupled with the surface amino group of the IDA substrate in a condensation reaction. Compared with conventional lithographic methods, this immobilization approach offers critical advantages, such as mild reaction conditions and a simple process for the successful integration of CP nanomaterials into the electrode substrate.[13] The hOR2AG1 contains terminal amine groups on cysteine (Cys) residues. Therefore, the covalent anchoring of hOR2AG1 on the nanotube surface

[*] S. H. Lee, H. S. Song, E. H. Oh, Prof. T. H. Park
School of Chemical and Biological Engineering
Institute of Bioengineering, Seoul National University
599 Gwanangno, Gwanakgu, Seoul 151-742 (Korea)
Fax: (+82) 2-875-9348
E-mail: thpark@plaza.snu.ac.kr
Dr. H. Yoon, O. S. Kwon, Prof. J. Jang
School of Chemical and Biological Engineering
Seoul National University
599 Gwanangno, Gwanakgu, Seoul 151-742 (Korea)
Fax: (+82) 2-888-1604
E-mail: jsjang@plaza.snu.ac.kr
Homepage: http://plaza.snu.ac.kr/~jsjang

Wiley
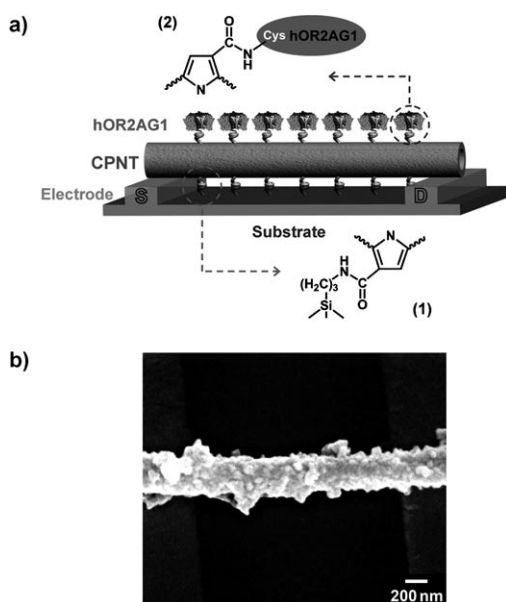InterScience®
DISCOVER SOMETHING GREAT

a)

b)

Figure 1. The hOR2AG1-conjugated CPNT FET platform: a) Schematic illustration. Only one nanotube is shown for clarity; covalent attachments (1) and (2) were used to bind CPNTs on the electrode substrate and to immobilize hORs to the nanotube, respectively. b) Typical FE-SEM image of a hOR2AG1-conjugated CPNT.

a)

b)

c)

Figure 2. a) Current–voltage curves of CPNTs on the electrode substrate before and after hOR immobilization in air (scan rate $= 10\ \mathrm{mV\,s^{-1}}$). b) Schematic diagram of a liquid–ion gate FET using hOR2AG1-conjugated CPNTs. c) Cyclic I_{SD}–E_G curve of the FET sensor based on 1OR-CPNTs measured in phosphate buffer at $\pm 10\ \mathrm{mV\,s^{-1}}$.

could be achieved through a similar condensation reaction. Figure 1b displays a typical field-emission scanning electron microscopy (FE-SEM) image of hOR2AG1-conjugated CPNTs deposited on the electrode substrate. It was clearly observed that the nanotube surface was made considerably more rugged by the attached hOR2AG1. Furthermore, there was no hOR on the electrode substrate except on the nanotubes, thus indicating that the hOR was selectively deposited on the nanotubes through chemical coupling.

Compared with a noncovalent approach, covalent anchoring provides better stability for analyte sensing in the liquid phase and further offers the possibility to control the chemical functionality of the nanotubes.[14] Under our experimental conditions, controlled loading of hOR2AG1 on the nanotube surface was achieved by adjusting its feeding amount in the coupling reaction. CPNTs were functionalized with hOR2AG1-to-CPNT weight ratios of 1:4 (1OR-CPNT), 1:2 (2OR-CPNT), and 1:1 (4OR-CPNT). Figure 2a exhibits current–voltage (*I–V*) curves of pristine CPNTs and hOR2AG1-conjugated CPNTs deposited on the electrode substrate.

The d*I*/d*V* value of CPNTs gradually decreased with increasing amount of conjugated hOR.[2] However, the ohmic contact was retained after the coupling reaction and washing process. This result means that the covalent immobilization of CPNTs on the electrode substrate resulted in reliable electrical contact. The recognition of odorants was carried out in solution. A liquid–ion gate FET geometry was constructed using a phosphate-buffered solution (10 mM, pH 7.4; Figure 2b).[12,13,15] The Ag/AgCl reference electrode and platinum counterelectrode were immersed in a buffered aqueous solution to provide gate control. Compared with conventional back gating, the liquid–ion gating is advanta-
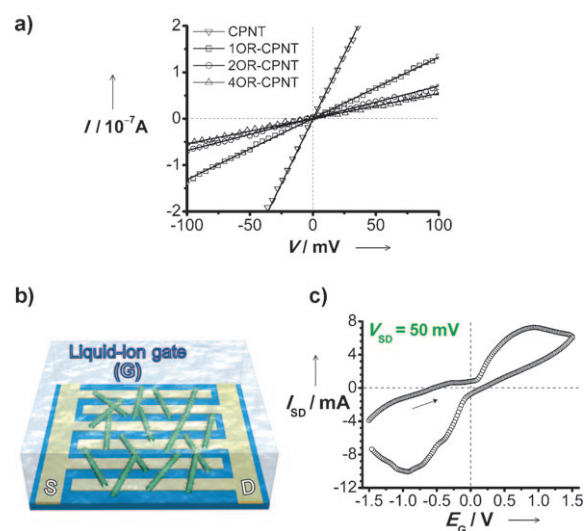
geous in making intimate contact with the nanotubes. To evaluate the FET characteristics, the gate potential (E_G) was applied between the reference electrode and the source electrode through the buffer solution. The source–drain current (I_{SD}) was modulated with varying E_G at a constant V_{SD} (50 mV), as shown in Figure 2c. The oxidation and reduction potentials of the CPNT were observed around $+0.9$ and -1.0 V.

The principal function of hOR proteins is to bind specific odorants and in turn to transduce a signal.[6] Such hOR–odorant interaction can affect the charge-carrier density of conjugated CP nanotubes, and thus it may allow label-free recognition of target odorants on the FET configuration. To investigate the sensing capability of hOR2AG1-conjugated CPNT FETs, the I_{SD} was monitored in real time at $V_{SD} = 50\ \mathrm{mV}$ ($E_G = 50\ \mathrm{mV}$), a low operating voltage, upon addition of odorants. It is known that hOR2AG1 specifically responds to amyl butyrate, a common reagent for fruit flavor.[16] Figure 3a displays the response of 1OR-CPNT FETs to the target odorant, amyl butyrate. The FET showed a concentration-dependent increase in I_{SD} when exposed to amyl butyrate. The I_{SD} increase was not attributed to electrochemical oxidation of amyl butyrate, because the applied E_G was well below its oxidation potential. It is believed that the current increase is due to a change in the charge-transport behavior of the CPNTs elicited by the hOR–odorant binding event. Specifically, the cysteine residues of hORs adopt an uncharged (RSH) state or a negatively charged (RS$^-$) state, associated with the acid-to-base transition of the sulfhydryl group.[6] Importantly, the specific binding of odorants initiates the structural rearrangement of hORs, finally leading to a relative increase in negatively charged base state (RS$^-$). The increased negative charge density at the hOR2AG1–CPNT interface can induce a p-type doping effect in the nanotubes,
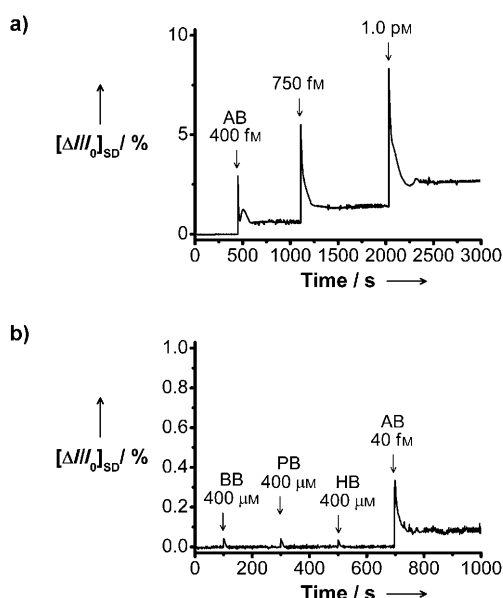
Figure 3. Real-time responses of 1OR-CPNT FET sensors measured at $V_{SD} = 50$ mV. Normalized I_{SD} changes upon addition of a) target odorant (amyl butyrate, AB) and b) nontarget (butyl butyrate, BB; propyl butyrate, PB; hexyl butyrate, HB) and target odorants.

which is probably responsible for the increase in I_{SD}. Figure 3b represents the selective response of the FET toward a particular odorant of interest. Other odorants such as propyl butyrate, butyl butyrate, and hexyl butyrate were employed as nontargets to verify the specificity of hOR2AG1–conjugated CPNTs. Upon addition of the nontargets, no significant changes in I_{SD} were observed, in contrast with the case of amyl butyrate. Consequently, it was evident that hOR2AG1-conjugated CPNTs had the outstanding ability to translate and amplify hOR–odorant interaction into a detectable signal as the transducer.

As mentioned above, the loading amount of hOR2AG1 on CPNTs was controlled during the covalent functionalization process. The hOR2AG1 near the CPNT acted as an effective gate, resulting in modulation of I_{SD}. Accordingly, the loading amount of hOR2AG1 is considered to be an important factor that affects the FET response. Figure 4 shows the dependence of the FET response on the amount of conjugated hOR. The detection limits of the FETs were found to be tens of femtomoles, approximately two orders of
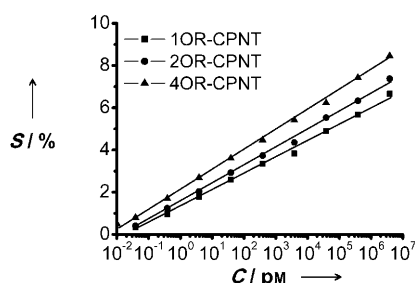

Figure 4. Calibration curves of the FET sensors. Sensitivity changes were plotted on a log scale (x axis) as a function of amyl butyrate concentration.

magnitude lower than those of existing bioelectronic noses.[8] The sample with the highest degree of functionalization, 4OR-CPNT, had the lowest detection limit (10 fM) as a result of the enhanced hOR–odorant interaction. The sensitivity was determined from the normalized I_{SD} change recorded after the addition of amyl butyrate. In all cases, the sensitivity increased linearly with the odorant concentration on the log-scale x axis. The sensitivity was in the order of 1OR-CPNT < 2OR-CPNT < 4OR-CPNT over a wide concentration range. In particular, at low concentrations (femtomole level), the sensitivity of 4OR-CPNT was approximately twice that of 1OR-CPNT or 2OR-CPNT. Therefore, it is expected that the sensitivity of the CPNT FET sensor can be tuned by careful control of the hOR loading.

In conclusion, we have demonstrated the feasibility of FET-type bioelectronic noses using hOR-conjugated CP nanotubes as the transistor channel and sensitive element. Our chemical immobilization strategy enabled the facile fabrication of the CPNT FET substrate with excellent electrical properties as well as the quantitative control of hOR functionalization. The FETs showed the possibility of specific odorant detection and gave measurable signals down to concentrations as low as tens of femtomoles. Considering these facts, the hOR-conjugated CP nanotube FET system offers a new direction for the highly sensitive and selective recognition of odorants and could be expanded to allow the multiplexed detection of various odorants after a judicious optimization.

Experimental Section

First, hOR2AG1 was expressed in *E. coli* as a fusion protein. The GST tag was used as a fusion partner. CPNTs were prepared by chemical oxidation copolymerization of pyrrole and P3CA with the aid of reverse-cylindrical micelles consisting of sodium bis(2-ethylhexyl)-sulfosuccinate. An efficient condensing agent, 4-(4,6-dimethoxy-1,3,5-triazin-2-yl)-4-methylmorpholinium chloride (DMT-MM), was synthesized according to the reported procedure.[17] The related experimental details are described in the Supporting Information.

An IDA was patterned on a glass substrate by a lithographic process. To construct the FET platform, in the first stage the IDA substrate was treated with 5 wt% aqueous APS for 6 h and then exposed to a mixture of 1 wt% CPNT in ethanol (10 µL) and 1 wt% DMT-MM in ethanol (10 µL) for 12 h. The resulting CPNT-immobilized substrate was rinsed with distilled water. Subsequently, the coupling reaction to attach hOR2AG1 to the CPNT surface was carried out using a mixture of hOR2AG1 and 1 wt% aqueous DMT-MM (10 µL) for 12 h. The feeding amounts of hOR2AG1 were 1:4, 2:4, and 4:4 (w/w) relative to CPNT for 1OR-CPNT, 2OR-CPNT, and 4OR-CPNT samples, respectively. Afterwards, the substrate was rinsed with distilled water and dried with a stream of nitrogen gas.

All electrical measurements were conducted with a Keithley 2400 sourcemeter and a Wonatech WBCS 3000 potentiostat. A solution chamber (50 µL volume) was designed and used for solution-based measurements. The current change was normalized as $\Delta I/I_0 = (I-I_0)/I_0$, where I_0 is the initial current and I is the measured real-time current.

[1] a) J. Jang, *Adv. Polym. Sci.* **2006**, *199*, 189–259; b) H. Yoon, M. Choi, K. J. Lee, J. Jang, *Macromol. Res.* **2008**, *16*, 85–102.

[2] a) H. Korri-Youssoufi, F. Garnier, P. Srivastava, P. Godillot, A. Yassar, *J. Am. Chem. Soc.* **1997**, *119*, 7388–7389; b) F. Garnier, H. Korri-Youssoufi, P. Srivastava, A. Yassar, *J. Am. Chem. Soc.* **1994**, *116*, 8813–8814; c) F. Garnier, *Angew. Chem.* **1989**, *101*, 529–533; *Angew. Chem. Int. Ed. Engl.* **1989**, *28*, 513–517.

[3] a) S. Hou, S. Wang, Z. T. F. Yu, N. Q. M. Zhu, K. Liu, J. Sun, W. Y. Lin, C. K. F. Shen, X. Fang, H. R. Tseng, *Angew. Chem.* **2008**, *120*, 1088–1091; *Angew. Chem. Int. Ed.* **2008**, *47*, 1072–1075; b) W. Wang, C. Alexander, *Angew. Chem.* **2008**, *120*, 7921–7924; *Angew. Chem. Int. Ed.* **2008**, *47*, 7804–7806.

[4] a) J. Jang, M. Chang, H. Yoon, *Adv. Mater.* **2005**, *17*, 1616–1620; b) H. Yoon, M. Chang, J. Jang, *Adv. Funct. Mater.* **2007**, *17*, 431–436; c) H. Yoon, J. Jang, *Mol. Cryst. Liq. Cryst.* **2008**, *491*, 21–31.

[5] a) F. Röck, N. Barsan, U. Weimar, *Chem. Rev.* **2008**, *108*, 705–725; b) M. Blaschke, T. Tille, P. Robertson, S. Mair, U. Weimar, H. Ulmer, *IEEE Sens. J.* **2006**, *6*, 1298–1308.

[6] a) I. Gaillard, S. Rouquier, D. Giorgi, *Cell. Mol. Life Sci.* **2004**, *61*, 456–469; b) H. Breer, *Anal. Bioanal. Chem.* **2003**, *377*, 427–433.

[7] a) M. S. Freund, N. S. Lewis, *Proc. Natl. Acad. Sci. USA* **1995**, *92*, 2652–2656; b) N. S. Lewis, *Acc. Chem. Res.* **2004**, *37*, 663–672; c) T.-Z. Wu, Y.-R. Lo, *J. Biotechnol.* **2000**, *80*, 63–73; d) W. Göpel, *Sens. Actuators B* **1998**, *52*, 125–142.

[8] a) H. J. Ko, T. H. Park, *Biosens. Bioelectron.* **2008**, *23*, 1017–1023; b) J. H. Sung, H. J. Ko, T. H. Park, *Biosens. Bioelectron.* **2006**, *21*, 1981–1986.

[9] a) R. A. Potyrailo, *Angew. Chem.* **2006**, *118*, 718–738; *Angew. Chem. Int. Ed.* **2006**, *45*, 702–723; b) S. W. Thomas III, G. D. Joly, T. M. Swager, *Chem. Rev.* **2007**, *107*, 1339–1386; c) V. Maheshwari, R. Saraf, *Angew. Chem.* **2008**, *120*, 7926–7945; *Angew. Chem. Int. Ed.* **2008**, *47*, 7808–7826; d) F. Wang, Y. Yang, T. M. Swager, *Angew. Chem.* **2008**, *120*, 8522–8524; *Angew. Chem. Int. Ed.* **2008**, *47*, 8394–8396.

[10] See several reviews regarding FET sensors: a) D. R. Kauffman, A. Star, *Angew. Chem.* **2008**, *120*, 6652–6673; *Angew. Chem. Int. Ed.* **2008**, *47*, 6550–6570; b) I. Willner, M. Zayats, *Angew. Chem.* **2007**, *119*, 6528–6538; *Angew. Chem. Int. Ed.* **2007**, *46*, 6408–6418.

[11] a) J. Jang, H. Yoon, *Langmuir* **2005**, *21*, 11484–11489; b) J. Jang, H. Yoon, *Chem. Commun.* **2003**, 720.

[12] a) G. P. Kittlesen, H. S. White, M. S. Wrighton, *J. Am. Chem. Soc.* **1984**, *106*, 7389–7396; b) H. S. White, G. P. Kittlesen, M. S. Wrighton, *J. Am. Chem. Soc.* **1984**, *106*, 5375–5377.

[13] a) H. Yoon, J. H. Kim, N. Lee, B. G. Kim, J. Jang, *ChemBioChem* **2008**, *9*, 634–641; b) H. Yoon, S. Ko, J. Jang, *J. Phys. Chem. B* **2008**, *112*, 9992–9997.

[14] S. Ko, J. Jang, *Biomacromolecules* **2007**, *8*, 182–187.

[15] M. M. Alam, J. Wang, Y. Guo, S. P. Lee, H. R. Tseng, *J. Phys. Chem. B* **2005**, *109*, 12777–12784.

[16] E. M. Neuhaus, A. Mashukova, W. Zhang, J. Barbour, H. Hatt, *Chem. Senses* **2006**, *31*, 445–452.

[17] M. Kunishima, C. Kawachi, K. Hioki, K. Terao, S. Tani, *Tetrahedron* **2001**, *57*, 1551–1558.